Morphological and biomolecular evidence for tuberculosis in 8th century AD skeletons from Bélmegyer-Csömöki domb, Hungary

Molnár, Erika; Donoghue, Helen D.; Lee, Oona Y.-c.; Wu, Houdini H.t.; Besra, Gurdyal S.; Minnikin, David E.; Bull, Ian D.; Llewellyn, Gareth; Williams, Christopher M.; Spekker, Olga; Pálfi, György

[Link to publication on Research at Birmingham portal](#)

Accepted Manuscript

Morphological and biomolecular evidence for tuberculosis in 8th century AD skeletons from Bélmegyer-Csömöki domb, Hungary

Erika Molnár, Helen D. Donoghue, Oona Y-C. Lee, Houdini H.T. Wu, Gurdyal S. Besra, David E. Minnikin, Ian D. Bull, Gareth Llewellyn, Christopher M. Williams, Olga Spekker, György Pálfi

1 **Morphological and biomolecular evidence for tuberculosis in 8th century AD skeletons from**

2 **Bélmegyer-Csömöki domb, Hungary**

3

4 Erika Molnár[a]*, Helen D. Donoghue[b], Oona Y-C. Lee[c], Houdini H.T. Wu[c], Gurdyal S. Besra[c],

5 David E. Minnikin[c], Ian D. Bull[d], Gareth Llewellyn[e], Christopher M. Williams[e], Olga Spekker[a] and

6 György Pálfi[a]

7

8

9 [a] Department of Biological Anthropology, University of Szeged, Szeged, Hungary

10 [b] Centre for Clinical Microbiology and Centre for the History of Medicine, University College

11 London, London, UK

12 [c] Institute of Microbiology and Infection, School of Biosciences, University of Birmingham,

13 Edgbaston, Birmingham, UK

14 [d] Organic Geochemistry Unit, School of Chemistry, University of Bristol, Bristol, UK

15 [e] National Mass Spectrometry Service Centre, School of Medicine, Grove Building, Swansea

16 University, Swansea, UK

17

18

19 Email addresses:

20 balinte@bio.u-szeged.hu; h.donoghue@ucl.ac.uk; o.y.lee@bham.ac.uk; h.wu.2@bham.ac.uk;

21 g.besra@bham.ac.uk; d.e.minnikin@bham.ac.uk; ian.d.bull@bristol.ac,uk;

22 g.llewellyn@swansea.ac.uk; christopher.matthew.williams@swansea.ac.uk;

23 olga.spekker@gmail.com; palfigy@bio.u-szeged.hu

24   *Corresponding author:

25   H-6724, Szeged

26   Közép fasor 52.

27   E-mail : balinte@bio.u-szeged.hu

28   Fax/Telephone : +36 62 544 314

29   Word count summary : 184

30   Word count (excluding summary and references) : 3075

31

32 **Summary**

33 Macromorphological analysis of skeletons, from 20 selected graves of the 8th century AD

34 Bélmegyer-Csömöki domb, revealed 19 cases of possible skeletal tuberculosis. Biomolecular

35 analyses provided general support for such diagnoses, including the individual without pathology,

36 but the data did not show coherent consistency over the range of biomarkers examined.

37 Amplification of ancient DNA fragments found evidence for the *Mycobacterium tuberculosis*

38 complex DNA only in five graves. In contrast, varying degrees of lipid biomarker presence were

39 recorded in all except two of the skeletons, though most lipid components appeared to be somewhat

40 degraded. Mycobacterial mycolic acid biomarkers were absent in five cases, but the weak, possibly

41 degraded profiles for the remainder were smaller and inconclusive for either tuberculosis or leprosy.

42 The most positive lipid biomarker evidence for tuberculosis was provided by mycolipenic acid, with

43 13 clear cases, supported by five distinct possible cases. Combinations of mycocerosic acids were

44 present in all but three graves, but in one case a tuberculosis-leprosy co-infection was indicated. In

45 two specimens with pathology, no lipid biomarker evidence was recorded, but one of these

46 specimens provided *M. tuberculosis* complex DNA fragments.

47

50

1. Introduction

The macromorphological diagnosis of skeletal tuberculosis (TB) in human remains is based upon the detection of secondary skeletal lesions.[1] The most common representation of skeletal TB is spondylitis tuberculosa, which affects the vertebral column. After vertebral involvement, the second most frequent alteration in TB is arthritis of the large, weight-bearing joints.[2] Initially, the diagnosis of TB in osteoarchaeological samples focused only on these classical TB lesions, representing a fairly developed stage of tuberculosis. However, TB may have affected many individuals without classical pathological changes, thus patients died in an earlier stage of tuberculosis long before these symptoms could have developed. Clearly, this early-stage TB is not recognizable on the basis of classical TB alterations, so if we consider only individuals with visible TB-related lesions, it is likely this will significantly underestimate the prevalence of tuberculosis in the examined historical populations.[1,3]

Because of the problems of tuberculosis diagnostics, the importance of establishing diagnostic criteria for early-stage TB became recognized in the late 20th century. A number of studies – mainly based on the examination of skeletal collections with known causes of death – have focused on searching for atypical or early-stage lesions in connection with tuberculosis infection. These investigations enabled the recognition of three types of atypical or early-stage TB alterations: rib lesions, superficial vertebral changes including hypervascularisation, and endocranial alterations.[3-7] Positive correlations between tuberculosis and stress indicators, such as long bone periostitis, *cribra orbitalia* and *cribra cranii*, were also recognized.[7,8] Since the 1990s, the identification of skeletal tuberculosis in ancient human remains has been facilitated by the confirmation of atypical or early-stage TB lesions by new biomolecular methods based on mycobacterial ancient DNA (aDNA) and lipid biomarker analyses.[1,9-12]

4

74   In 1990, the first paleopathological analyses of the 8th century AD series Bélmegyer-Csömöki

75   domb were essentially based on macromorphological and radiological examinations, biomolecular

76   methods were used only in a few cases. From a macromorphological point of view, those

77   investigations only considered classical TB alterations.[9,13,14,15] An advanced-age female skeleton

78   from the grave No. 65 showed severe osteolytic lesions of the anterior portion of the thoracic and

79   lumbar vertebral bodies, causing an unequal collapse, which led to angular kyphosis (Suppl. Fig. S1

80   a-b).[14] Mycobacterial DNA targets IS*6110* and the 65-kDa antigen gene, of the *Mycobacterium*

81   *tuberculosis* complex (MTBC), were found in samples from this specimen.[9] In another case, of a

82   mature male individual (grave No. 90), the pathological remodelling and fusion of the lumbosacral

83   region and the irregular *ante-mortem* erosion on the ventral surface of the sacrum, support the

84   diagnosis of a lumbo-sacral tuberculous involvement with cold abscess. In addition, the severe

85   destruction both of the left hip bone and proximal femur is suggestive of tuberculous arthritis or

86   *coxitis tuberculosa* (Suppl. Fig. S1 c-d).[15] The diagnosis of skeletal TB was confirmed by

87   biomolecular results, the identification of the DNA-fragment (65-kDa antigen gene) of the MTBC

88   was successful.[9] In a further case, the complete ankylosis of the right knee indicated *gonitis*

89   *tuberculosa* of an elderly male individual from grave No. 215.[13]

90   Marcsik and co-workers published two further classical TB cases in 2007.[16] A young female

91   skeleton from grave No. 38 exhibited signs of probable tuberculous arthritis (*coxitis tuberculosa*) of

92   the right hip joint. Skeletal remains of an adult male individual (grave No. 189) presented complete

93   ankylosis of the 9th and 10th thoracic vertebrae and fusion of the 1st and 2nd and the 3rd and 4th

94   lumbar vertebrae. In addition, new bone formation and osteophytes were found on the ventral

95   surfaces of all lumbar vertebral bodies. These alterations suggest the diagnosis of spondylitis

96   tuberculosa.[16]

97   The above mentioned former investigations of the series from the Bélmegyer-Csömöki domb

98   have provided interesting paleopathological cases of skeletal tuberculosis. However, the complete

5

99   skeletal material has never been analysed systematically for both classical and early-stage TB

100   lesions, and biomolecular analyses had been undertaken only in a few cases. The recent

101   development of diagnostic criteria in the field of paleopathology of TB and biomolecular methods

102   for detection of the MTBC encouraged us to perform a re-examination of the series from 2009. The

103   aim of this study is to summarize the results of this re-examination.

104   **2. Material and Methods**

105   *2.1 Archaeological background*

106   The skeletal material for this study derives from the archaeological site of the Bélmegyer-

107   Csömöki domb, rising about three kilometres south-east of the village Bélmegyer, in South-Eastern

108   Hungary. During a long-running excavation (1985 – 1989), skeletal remains of 240 individuals

109   were unearthed. On the basis of the grave goods found in the completely excavated cemetery, it was

110   used for burials between 670 – 800 AD during the late Avar Period.[17,18]

111   Our research strategy was to combine different diagnostic methods in order to get independent

112   verification using different biomarkers. First we conducted the morphological analysis of the

113   skeletal series. Next, bone samples were taken from the skeletal remains of the suspected TB cases.

114   Small pieces from the same rib were selected and sent to separate centres for the aDNA and lipid

115   biomarker analyses.

116   *2.2 Macromorphological analysis*

117   The paleopathological examination of the mostly well-preserved skeletal remains of the 240

118   individuals (95 males, 72 females, 73 undeterminable) was carried out in the Department of

119   Biological Anthropology, University of Szeged, Hungary. These investigations were performed

120   using macromorphological methods, focussing on previously detailed classical[2] and atypical TB

121   alterations.[3-7]

122   *2.3 Mycobacterial aDNA analysis*

123   2.3.1 Mycobacterial DNA extraction

124   Possible cases of skeletal TB, defined according to skeletal morphological alterations, were

125   examined for the presence of aDNA from the *Mycobacterium tuberculosis* complex (MTBC).

126   Recommended protocols for aDNA work were followed[19] with separate rooms and equipment for

127   different stages of the process. Well-established methods were employed for aDNA extraction and

128   amplification[20-27] as detailed in Donoghue *et al* in this volume[28] and in Supplementary data. The

129   approach used was of a slow but thorough period of sample disruption, one aliquot treated with N-

130   phenacylthiozolium bromide (PTB), to cleave any covalent cross-links thus facilitating DNA strand

131   separation and amplification.[21] Subsequently, samples were treated with guanidium thiocyanate,

132   followed by sample and bacterial cell disruption, using boiling and snap-freezing in liquid nitrogen.

133   All fractions of the sample were used in the extraction. DNA was captured with silica and the

134   pelletswashed and dried.[28] Silica supernates from PTB-negative samples were also processed by

135   removal of protein followed by DNA precipitation with isopropanol ($-20\ ^{o}$C).[28] Dried samples were

136   re-hydrated with elution buffer and used immediately or stored at $-20\ ^{o}$C. Negative extraction

137   controls were processed in parallel with the test samples.

138   2.3.2 DNA amplification and detection

139   Two specific regions of the *M. tuberculosis* complex were targeted – the repetitive elements

140   IS*6110* (1–25 copies/cell) and IS*1081* (6 copies/cell). The IS*6110* primers used for conventional

141   PCR had a target region of 123 bp[22] and the IS*1081* primers produce an amplicon of 113 bp.[23]

142   Later, specific *M. tuberculosis* primers and a fluorescent probe were used[24] to enable shorter DNA

143   fragments to be detected in a real-time PCR reaction (Supplementary data).

144   2.3.3 The PCR conditions

145   The PCR mix included 2mM bovine serum albumin to reduce PCR inhibition[25] and 2.0mM

146   MgCl$_2$. PCR assays were initially run at an annealing temperature of 58°C and amplified DNA was

147 examined by agarose gel electrophoresis.[26] Subsequently, amplification was performed in a final

148 volume of 25µl using a RotorGene[©] 3000 (Qiagen) real-time platform[27] to enable the detection of

149 DNA using SYBR Green and melt analysis or specific primers with fluorescent probe. Annealing

150 was at 60°C. A hot-start *Taq* polymerase was used to minimize non-specific primer and template

151 binding. Negative DNA extraction and PCR controls were processed alongside the test samples.

152 *2.4 Lipid Biomarker Analysis*

153 Details of the methods and analysis are given in the Supplementary data. Specimens were

154 hydrolysed by heating with 30% potassium hydroxide in methanol (2ml) and toluene (1ml) at 100°C

155 overnight.[11,29] In parallel, standard biomass of *M. tuberculosis* and *M. leprae* was processed. Long-

156 chain compounds were extracted as described previously[29] and the extract was treated with

157 pentafluorobenzyl bromide, under phase-transfer conditions[11,29] to convert acidic components into

158 pentafluorobenzyl (PFB) esters. Subsequent separation on an Alltech 209250 (500mg) normal phase

159 silica gel cartridge gave fractions containing non-hydroxylated fatty acid PFB esters, mycolic acid

160 (MA) PFB esters and free phthiocerols.[11,29] The MA PFB esters reacted with pyrenebutyric acid

161 fi(PBA) to produce PBA-PFB MA derivatives, which were purified on an Alltech 205250 (500mg)

162 C_{18} reverse phase cartridge.[11,29] The PBA-PFB mycolates were analysed by reverse phase HPLC,

163 as described previously.[11,29] The non-hydroxylated PFB ester fractions were refined on an Alltech

164 205250 (500mg) reverse phase silica gel cartridge, using a water-methanol/methanol/methanol-

165 toluene elution sequence.[29] A fraction enriched in mycocerosic acid and other longer chain (> C20)

166 PFB esters was eluted by 100% methanol with the more usual C_{12} to C_{20} esters eluting in the earlier

167 water/methanol fractions. The fractions containing possible mycocerosates, were analysed by

168 negative ion chemical ionization gas chromatography mass spectrometry (NICI-GCMS), as

169 previously described.[29]

170 **3. Results**

171 *3.1 Macromorphological analysis*

172 During the macromorphological analysis of the skeletal material of the Bélmegyer-Csömöki

173 domb, 19 cases of probable skeletal tuberculosis were detected. Classical TB changes were

174 observed in the five cases detailed above in the Introduction (Suppl. Fig. S1 a-d; Table 1), while

175 atypical or early-stage TB lesions were observed in a further 14 cases (Suppl. Fig. S2 a-c; Table 1).

176 It is clear, therefore, that these atypical or early TB changes occurred significantly more often than

177 the classical alterations. Only grave No. 86 showed no macromorphological evidence of

178 tuberculosis (Table 1).

179 The most frequent lesions were periosteal reactions on the visceral rib surfaces and abnormal

180 vertebral vascularisation. Ten cases of superficial vertebral changes were detected (Table 1). With

181 the exception of three specimens (two mature males and one elderly female), the affected

182 individuals belong to younger age groups: one Infans II, three juveniles and three young adult

183 males. Eight individuals exhibited hypervascularisation of the anterior aspect of vertebral bodies,

184 while lytic vertebral lesions were revealed in only two cases.

185 As for rib changes, eight individuals (one juvenile, four adults, two mature and one elderly)

186 showed signs of periosteal appositions on the visceral costal surfaces (Table 1). In the majority of

187 the cases, rib periostitis showed a woven-remodelled character, indicating a less active process

188 generating these pathological changes. In two other cases (grave No. 17 and grave No. 212) it was

189 noticed that the visceral surfaces of ribs had a roughened texture.

190 Endocranial alterations were revealed in five individuals only (Table 1). Except for a mature

191 male specimen (grave No. 33), the affected individuals represent younger age groups: one juvenile

192 and three young adults (one male and two females). Concerning lesion morphology, abnormal

193 blood vessel impressions on the internal surface of the skull were observed in three of the five

194 cases, though the endocranial lamina of grave No. 22 exhibited small granular impressions similar

195 to those described by Schultz[5] and in the skeleton of a young adult female individual (grave No.

196 233) *serpens endocrania symmetrica* (SES) was identified.

197   With the exception of two cases (grave No. 88 and grave No. 188), an association of different

198 alterations could be detected. Atypical or early-stage TB changes were accompanied by stress

199 factors in a number of cases: *cribra orbitalia* (mainly the porotic form) was observed in seven

200 cases, while long bone periostitis occurred in six cases (Table 1). Long bone periostitis appeared

201 mostly on femora and tibiae, but in three cases the long bones of the upper extremities were also

202 affected.

203   *3.2 Biomolecular Analyses*

204   The aDNA amplification studies gave positive results for nine of the 20 graves investigated, but

205 for only one of the four "classical TB cases" (Table 1). Full data of the aDNA analysis are provided

206 in Supplementary data. Total mycolic acid (MA) profiles are recorded in Fig. 1 that also includes a

207 summary of the overall lipid biomarker and aDNA results. All the MA profiles were too weak to

208 allow further diagnostic analyses, by sequential normal and reverse phase HPLC.[11,29] Material from

209 five graves (Nos. 33, 66, 154, 188, 212) yielded no MAs. Fig. 2 shows three representative profiles

210 of mycolipenic (ML) and mycocerosic (MC) acids; full data are provided in Supplementary Figures

211 S3, S4 and S5.

212   The results of the lipid biomarker analyses could be placed into 6 groups (Table 1, Figs. S3-5).

213 Group 1 (grave Nos. 22, 86, 88, 134) had clear evidence of all three MA, ML and MC lipid

214 biomarker classes; grave No. 22, however, also included C_{33} and C_{34} mycocerosates, indicative of

215 leprosy. The major Group 2 (grave Nos. 12, 17, 48, 65, 90, 189, 215) was characterised by the

216 presence of a clear signal for mycolipenate (ML), with less convincing evidence for the other MA

217 and MC classes. Group 3 (grave Nos. 66, 188) had two representatives with good ML, weak MCs,

218 but no MA; a single member of Group 4 (grave No. 154) had only a poor ML signal. Four

219 representatives in Group 5 (grave Nos. 38, 92, 116, 233) provided weak inconclusive evidence for

220 ML and MC biomarkers. Final Group 6 (grave Nos. 33, 212) lacked any evidence of mycobacterial

221 lipid biomarkers. A close correlation with the aDNA data was not observed. Only one (grave No.

222 88) of four in the best Group 1 lipid class gave amplified DNA. Correlation was better for the

223 Group 2 lipid class with four of seven having aDNA. In the less strong or negative lipid Groups 3-6,

224 only one grave in each group had a positive aDNA result.

225 **4. Discussion and conclusions**

226 In 19 out of the 20 skeletons from Bélmegyer-Csömöki domb a range of macromorphological

227 changes, indicative of tuberculosis, were observed. Only nine of the 20 graves yielded *M.*

228 *tuberculosis* aDNA on amplification. Lipid biomarker evidence for *M. tuberculosis* was discerned

229 in all but two of the specimens, but the strength and conclusiveness of the lipid signals could be

230 allocated to five levels (Groups 1-5) (Fig. 2). Taken by themselves, the weak total mycolic acid

231 profiles (Fig. 2) cannot be regarded as positive evidence for ancient tuberculosis. The constituents

232 of the profiles are significantly smaller than those of standard *M. tuberculosis*, suggesting either

233 considerable degradation or the presence of environmental mycobacteria. The former alternative is

234 favoured, as the two specimens (grave Nos. 33, 212) that lacked any evidence of mycolipenate

235 (ML) and mycocerosate (MC) biomarkers (Table 1), showed no evidence of any mycolates (Fig. 2).

236 Given that assumption, the MA profiles provide background support for mycobacterial infection.

237 The most positive evidence for the presence of tuberculosis resides in the MLs, which were

238 found to be usually, as strong as, or stronger than the MCs, an exception being grave No. 88 with an

239 excellent MC profile. Indeed in grave No. 154 the only lipid biomarker evidence is a very weak ML

240 signal; this is probably genuine as aDNA was amplified from this sample.

241 Of five classical tuberculosis cases (Table 1) with skeletal alterations characteristic for advanced

242 stage TB, one only (grave No. 189) was positive for MTBC DNA with clear lipid biomarker

11

243   support (Fig. 2; Table 1). Four of the diagnosed classical TB cases were DNA negative. However,

244   in three of these negative cases (grave Nos. 65, 90, 215) the diagnosis of skeletal tuberculosis was

245   confirmed by lipid biomarker analysis with quite strong evidence (Fig. 2). For grave No. 38, lipid

246   biomarker data were weak.

247   For cases, showing atypical or early-stage TB lesions (Table 1), many of the biomarker results

248   were inconsistent. The best lipid profiles (Group. 1) were recorded for grave Nos. 22, 86, 88 and

249   134, but only the very fragmented material from grave No. 88 was supported by aDNA.

250   Interestingly, grave No. 22 appeared to be a co-infection with tuberculosis and leprosy, the former

251   being confirmed with a strong mycolipenate peak and the latter by C_{33} and C_{34} mycocerosates (Fig.

252   2). The next Group 2 lipid biomarker level, with clear ML backed up by MCs in seven graves (Nos.

253   12, 17, 48, 65, 90, 189, 215) was supported by aDNA in three atypical cases (grave Nos. 12, 17, 48)

254   in addition to the classical case in grave No. 189 (Table 1). Only one (grave No. 66) of the two

255   Group 3 biomarker level specimens had aDNA support, but both graves (Nos. 66, 188) had good

256   ML backed up by weak but clear MCs. Dropping down to the single lipid biomarker Group 4

257   representative (grave No. 154), as mentioned above, aDNA amplification was supported by a weak

258   but clear ML. The four graves (Nos. 38, 92, 116, 233) assigned to lipid Group 5 had only minimal

259   ML and MC evidence but aDNA was obtained from No. 92. Although grave No. 33 was MTBC

260   DNA positive, negative lipid profiles were recorded. A juvenile male (grave No. 212.) was the only

261   specimen showing atypical or early-stage TB lesions, where the biomolecular analyses gave

262   negative results for the presence of both MTBC DNA and lipid biomarkers. The presence of

263   mycolic acid biomarkers in material from grave No. 65 was previously suggested[30] but the scientific

264   basis for such a diagnosis has been dismissed.[31]

265   Morphological assessment, detection of ancient DNA and demonstration of M. tuberculosis

266   complex cell wall lipid markers proves there was widespread TB infection in this 8th century

267   population. A variety of lesions at different stages of development were observed. The biomolecular

268   studies confirmed the presence of tuberculosis and lipid analysis also indicated a TB/leprosy

269   coinfection. Our study highlights the difficulties of demonstrating TB in these individuals from over

270   1300 years ago and the importance of using different methods is very clear. The relative success of

271   lipid biomarkers compared with aDNA is probably due to their greater stability over time. This

272   underlines the complementarity of morphological, aDNA and lipid biomarkers analyses in the

273   diagnosis of ancient TB infections.

274   **Ethical approval**

275   Not required

276   **Funding**

284   **Author contributions**

285   EM and GP conceived the study and with OS performed the macromorphological analysis. HD

286   performed the aDNA studies. DM and GB conceived the lipid work, which was performed by OL,

287   HW, IB, GL and CW. The lipid data were analyzed by DM, GB, OL and HW. EM, DM and HD

288   wrote the manuscript and all authors approved the final version.

289   **Competing interests**

290   None declared.

291

13

References

1. Pálfi Gy, Bereczki Zs, Ortner DJ, Dutour O. Juvenile cases of skeletal tuberculosis from the Terry Anatomical Collection (Smithsonian Institution, Washington, D.C., USA). *Acta Biologica Szegediensis* 2012; **56**:1-12.

2. Ortner DJ. *Identification of paleopathological conditions in human skeletal remains*. San Diego: Academic Press, 2003.

3. Dutour O. Archaeology of human pathogens: palaeopathological appraisal of palaeoepidemiology. In: Raoult D, Drancourt M, editors. *Paleomicrobiology: past human infections*. Berlin, Heidelberg: Springer–Verlag GmbH, 2008. p. 125-144.

4. Baker BJ. Early manifestations of tuberculosis in the skeleton. In: Pálfi Gy, Dutour O, Deák J, Hutás I, editors. *Tuberculosis: past and present*. Szeged & Budapest: TB Foundation & Golden Book Publisher, 1999. p. 301-307.

5. Schultz M. Paleohistopathology of bone: a new approach to the study of ancient diseases. *Yearbook of Physical Anthropology* 2001; 44:106-147.

6. Hershkovitz I, Greenwald CM, Latimer B, Jellema LM, Wish-Baratz S, Eshed V, Dutour O, Rothschild BM. Serpens Endocrania Symmetrica (SES): a new term and a possible clue for identifying intrathoracic disease in skeletal populations. *American Journal of Physical Anthropology* 2002; 118:201-216.

7. Pálfi Gy. Paleoepidemiological reconstruction of tuberculosis with particular attention to Europe. In: Bennike P, Bodzsár E, Susanne C, eds. *Biennial Books of EAA* 2002;**2**:193-210.

8. Stuart-Macadam PL. Nutritional deficiency diseases: a survey of scurvy, rickets and iron deficiency anemia. In: Isçan MY, Kennedy KAR, editors. *Reconstruction of life from the skeleton*. New York: Alan R. Liss Publisher, 1989. p. 201-222.

9. Haas CJ, Zink A, Molnár E, Szeimies U, Reischl U, Marcsik A, Ardagna Y, Dutour O, Pálfi Gy, Nerlich AG. Molecular evidence for different stages of tuberculosis in ancient bone samples from Hungary. *American Journal of Physical Anthropology* 2000; 113: 293-304.

318 10. Zink AR, Molnár E, Motamedi N, Pálfi Gy, Marcsik A, Nerlich AG. Molecular history of

319 tuberculosis from ancient mummies and skeletons. *International Journal of Osteoarchaeology*

320 2007; 17:380-391.

321 11. Hershkovitz I, Donoghue HD, Minnikin DE, Besra GS, Lee OY-C, Gernaey AM, Galili E,

322 Eshed V, Greenblatt CL, Lemma E, Bar-Gal GK, Spigelman M. Detection and molecular

323 characterization of 9000-year-old *Mycobacterium tuberculosis* from a Neolithic settlement in

324 the Eastern Mediterranean. *PLoS ONE* 2008; 3:e3426.

325 12. Pósa A, Maixner F, Lovász G, Molnár E, Bereczki Zs, Perrin P, Zink AR, Pálfi Gy. Revision of

326 tuberculous lesions in the Bácsalmás-Óalmás series – preliminary morphological and

327 biomolecular studies. *Anthropologischer Anzeiger* 2012, doi: 10.1127/0003-5548/2012/0260.

328 13. Pálfi Gy, Csernus Z. Arthrite infectieuse ankylosante dans une série du VIIIe siècle en Hongrie.

329 *Paléobios* 1990; 6:37-41.

330 14. Pálfi Gy. The osteoarchaeological evidence of vertebral tuberculosis in the 8th century. *Acta*

331 *Biologica Szegediensis* 1991; 37:101-105.

332 15. Pálfi Gy, Marcsik A, Kovács J. Lumbosacral and hip tuberculosis in a Migration period

333 skeleton. *Journal of Paleopathology* 1992; 4:179-184.

334 16. Marcsik A, Molnár E, Ősz B. *Specifikus fertőző megbetegedések csontelváltozásai történeti*

335 *népesség körében*. Szeged: JatePress, 2007.

336 17. Medgyesi P. Késő avar temető Bélmegyer-Csömöki dombon (Előzetes jelentés).

337 Spätawarenzeitliches Gräberfeld auf Hügel Bélmegyer-Csömök (Vorbericht). In: *A Móra*

338 *Ferenc Múzeum Évkönyve*. Szeged: 1991. p. 241-256.

339 18. Medgyesi P. Bélmegyer. In: Jankovich BD, editor. *Magyarország régészeti topográfiája. 10.*

340 *Békés megye régészeti topográfiája.* Budapest: Akadémiai Kiadó, 1998. p. 342-348.

341 19. Taylor GM, Mays SA, Huggett JF. Ancient DNA (aDNA) studies of man and microbes:

342 general similarities, specific differences. *International Journal of Osteoarchaeology* 2010;

343 20:747-751.

344   20. Donoghue HD, Marcsik A, Matheson C, Vernon K, Nuorala E, Molto J, Greenblatt C,

345   Spigelman M. Co-infection of *Mycobacterium tuberculosis* and *Mycobacterium leprae* in

346   human archaeological samples—a possible explanation for the historical decline of leprosy.

347   *Proceedings of the Royal Society B: Biological Sciences* 2005; 272:389-394.

348   21. Poinar HN, Hofreiter M, Spaulding WG, Martin PS, Stankiewicz BA, Bland H, Evershed EP,

349   Possnert G, Pääbo S. Molecular coproscopy: dung and diet of the extinct ground sloth

350   *Nothrotheriops shastensis*. *Science* 1998; 281:402-406.

351   22. Eisenach KD, Cave MD, Bates JH, Crawford JT. Polymerase chain reaction amplification of a

352   repetitive DNA sequence specific for *Mycobacterium tuberculosis*. *The Journal of Infectious*

353   *Diseases* 1990; 161:977-981.

354   23. Taylor GM, Stewart GR, Cooke M, Chaplin S, Ladva S, Kirkup J, Palmer S, Young DB.

355   Koch's Bacillus—a look at the first isolate of *Mycobacterium tuberculosis* from a modern

356   perspective. *Microbiology* 2003; 149:3213-3220.

357   24. Évinger S, Bernert Zs, Fóthi E, Wolff K, Kővári I, Marcsik A, Donoghue HD, O'Grady J, Kiss

358   KK, Hajdu T. New skeletal tuberculosis cases in past populations from Western Hungary

359   (Transdanubia). *HOMO – Journal of Comparative Human Biology* 2011; 62:165-183.

360   25. Abu Al-Soud W, Rådström P. Effects of amplification facilitators on diagnostic PCR in the

361   presence of blood, feces and meat. *Journal of Clinical Microbiology* 2000; 38:4463-4470.

362   26. Hajdu T, Donoghue HD, Bernert Zs, Fóthi E, Kővári I, Marcsik A. A case of spinal

363   tuberculosis from the Middle Ages in Transylvania (Romania). *Spine* 2012; 37:e1598-1601.

364   27. Taylor GM, Worth DR, Palmer S, Jahans K, Hewinson RG. Rapid detection of *Mycobacterium*

365   *bovis* DNA in cattle lymph nodes with visible lesions using PCR. *BMC Veterinary Research*

366   2007; 3:12-22.

367   28. Donoghue HD, Spigelman M, O'Grady J, Szikossy I, Pap I, Lee OY-C, Wu HHT, Besra GS,

368   Minnikin DE. Ancient DNA analysis – an established technique in charting the evolution of

369   tuberculosis and leprosy. In: *Proceedings of ICEPT-2 – The Past & Present of Tuberculosis: a*

370   *multidisciplinary overview on the origin and evolution of TB. One of the Conference series on*

371   *the occasion of the 75th Anniversary of Albert Szent-Györgyi 's Nobel Prize Award, Szeged,*

372   *Hungary, 22nd – 25th March 2012.*

373   29. Lee OY-C, Wu HHT, Donoghue HD, Spigelman M, Greenblatt CL, Bull ID, Rothschild BM,

374   Martin LD, Minnikin DE, Besra GS. *Mycobacterium tuberculosis* complex lipid virulence

375   factors preserved in the 17,000-year-old skeleton of an extinct bison, *Bison antiquus. PLoS*

376   *ONE* 2012; 7:e41923.

377   30. Mark L, Patonai Z, Vaczy A, Lorand T, Marcsik A. High-throughput mass spectrometric

378   analysis of 1400-year-old mycolic acids as biomarkers for ancient tuberculosis infection. *J*

379   *Archaeol Sci*, 201037, 302–305.

380   31. Minnikin D, Lee OY-C, Wu HHT, Besra G, Donoghue H. Molecular biomarkers for ancient

381   tuberculosis. In: Cardona, P-J. (ed.) Understanding tuberculosis - deciphering the secret life of

382   the bacilli. Rijeka, Croatia: InTech Open Access Publisher 2012. p. 3–36. ISBN-13: 978-953-

383   307-946. Available from: http://www.intechopen.com/articles/show/title/molecular-

384   biomarkers-for-ancient-tuberculosis

385

386 **Figure legends**

387 Figure 1. Reverse phase fluorescence HPLC of total mycolates. The grave numbers are

388 accompanied (in brackets) by the amount of sample analysed (mg). The "Lipid" column indicates

389 the diagnostic power of mycolate (MA), mycolipenate (ML) and mycocerosate (MC) lipid

390 biomarkers: ++++ (group 1), clear evidence of MA, ML and MC; +++ (group 2), clear ML signal

391 with less strong MA and MC; ++ (group 3), good ML, weak MC and no MA; + (group 4), only a

392 clear weak ML peak; +? (group 5), weak inconclusive ML and MC with some MA support; **-**

393 (group 6), no evidence of mycobacterial lipids; ++++***,** strong *M. tuberculosis* lipid signals with

394 additional MC indicating *M. leprae*. The "aDNA" list records the presence of amplified DNA

395 fragments.

396 Figure 2. Representative selected ion monitoring (SIM) negative ion-chemical ionization gas

397 chromatography-mass spectrometry (NI-CI GC-MS) profiles of mycolipenate and mycocerosates.

398 **A, C, E** grave Nos. 88 (Bristol University), 134 and 22 (Swansea University); **B, C** *M. tuberculosis*

399 standard recorded at Bristol and Swansea, respectively; **F**, *M. leprae* standard recorded at Swansea.

400 Ions monitored are exemplified by C_{27} *m/z* 407 and C_{27} *m/z* 409, representing C_{27} mycolipenate and

401 C_{27} mycocerosate, respectively. Relative intensities **(bold in brackets)** are shown normalized to the

402 major component **(100)**.

403

404   **Table 1.** Data for material investigated from Bélmegyer-Csömöki domb.

CLASSICAL TB CASES

Gr No	sex	age at death	macromorphology			aDNA	lipid biomarkers		
			ST	CT	GT		MA	ML	MC
38	F	16□18	□	+	□	□	+	+?	+?
65	F	Maturus	+	□	□	□	+?	+	+
90	M	57□62	+	+	□	□	+	+	+?
189	M	25□28	+	□	□	+	+	+	+?
215	F	55□60	□	□	+	□	+?	+	+

ATYPICAL (EARLY-STAGE) TB CASES

Gr No	sex	age at death	macromorphology					aDNA	lipid biomarkers		
			SVC	RP	EL	LBP	CO		MA	ML	MC
12	M	33□39	□	+++	□	+	□	+	+?	++	+?
17	M	22□25	+	+	+	+	+	+	+?	++	+?
22	undet.	16□18	+	□	+	□	□	□	+	++	+
33	M	40□45	+	□	+	+	+	+	□	□	□
48	M	55□60	+	+	□	+ (DP)	□	+	+	+	+
66	F	61□67	+	+	□	□	□	+	□	+	+?
86	M	59□64	□	□	□	□	□	□	+	++	+
88	F	40□45	□	+++	□	□	□	+	+	+	+++
92	M	20□25	+	+++	□	+	□	+	+	+?	+?
116	F	25□30	□	+++	+	+++ (DP)	□	□	+	+?	+?
134	F	16□18	+	□	□	□	+	□	++	+	+
154	M	20□24	+	□	□	□	+	+	□	+?	□

19

188	undet.	7	+	☐	☐	☐	☐	☐	☐	++	+
212	M	18☐20	+	+	☐	☐	☐	☐	☐	☐	☐
233	F	23☐25	☐	☐	+	☐	☐	☐	+	+?	+?

405

406 **Gr No** = grave No; **F** = female; **M** = male; **undet.** = undeterminable sex; **ST** = spondylitis

407 tuberculosa; **CT** = coxitis tuberculosa; **GT** = gonitis tuberculosa; **SVC** = superficial vertebral

408 changes; **RP** = rib periostitis; **EL** = endocranial lesions; **LBP** = long bone periostitis; **CO** = cribra

409 orbitalia; **DP** = diffuse periostitis; **MA =** mycolates; **ML** = mycolipenate; **MC** = mycocerosates.
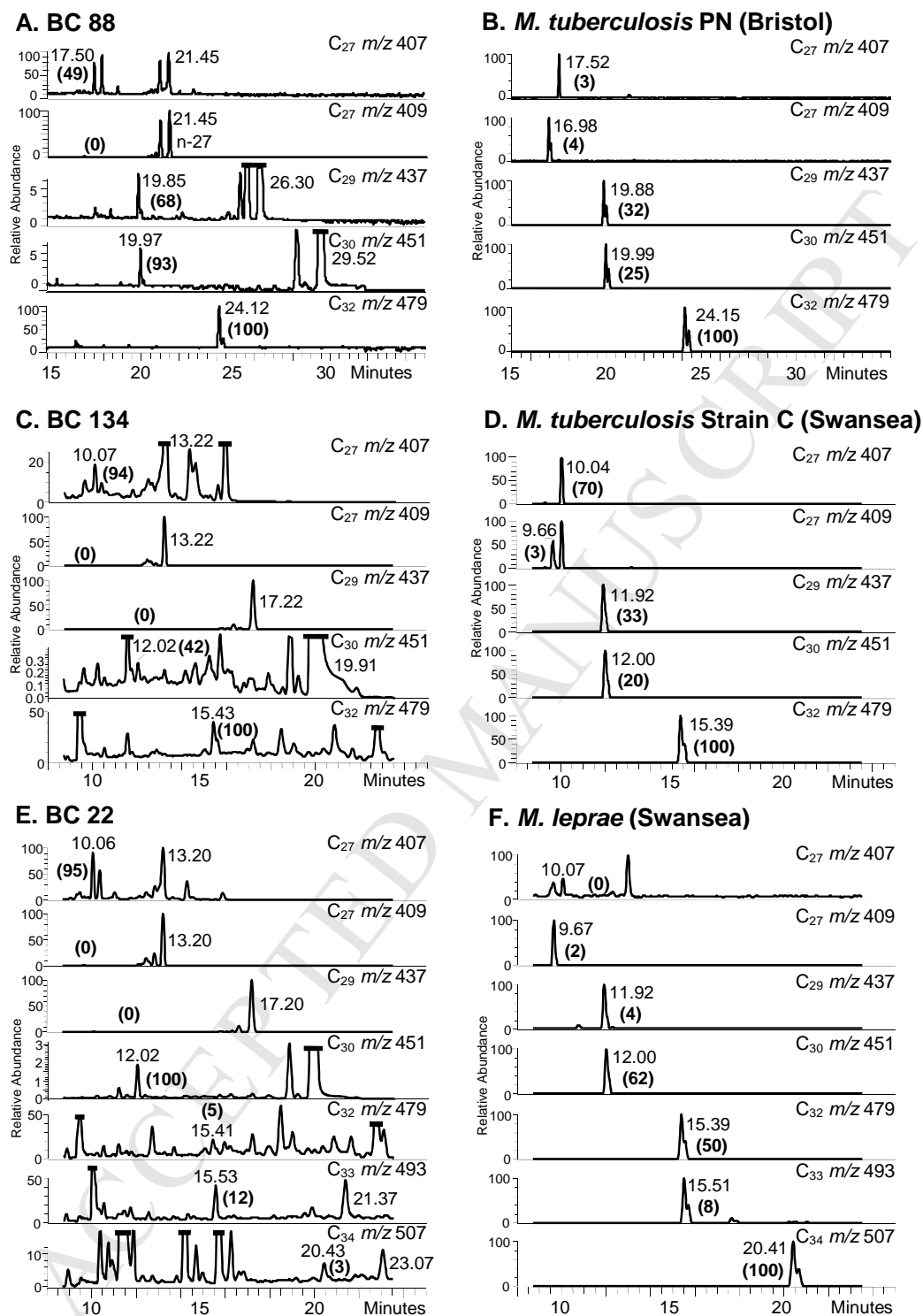
410

411   **Figure 1**

Reverse phase HPLC of total mycolates

Sample (mg)	Lipid	aDNA
BC 12 (608)	+++	+
BC 17 (836)	+++	+
BC 22 (989)	++++*	-
BC 33 (367)	-	+
BC 38 (507)	+?	-
BC 48 (866)	+++	+
BC 65 (759)	+++	-
BC 66 (817)	++	+
BC 86 (813)	++++	-
BC 88 (117)	++++	+
BC 90 (963)	+++	-
BC 92 (1180)	+?	+
BC 116 (924)	+?	-
BC 134 (1162)	++++	-
BC 154 (1040)	+	+
BC 188 (737)	++	-
BC 189 (964)	++++	+
BC 212 (1098)	-	-
BC 215 (1196)	+++	-
BC 233 (1053)	+?	-
M. tuberculosis		
M. leprae		
Blank		
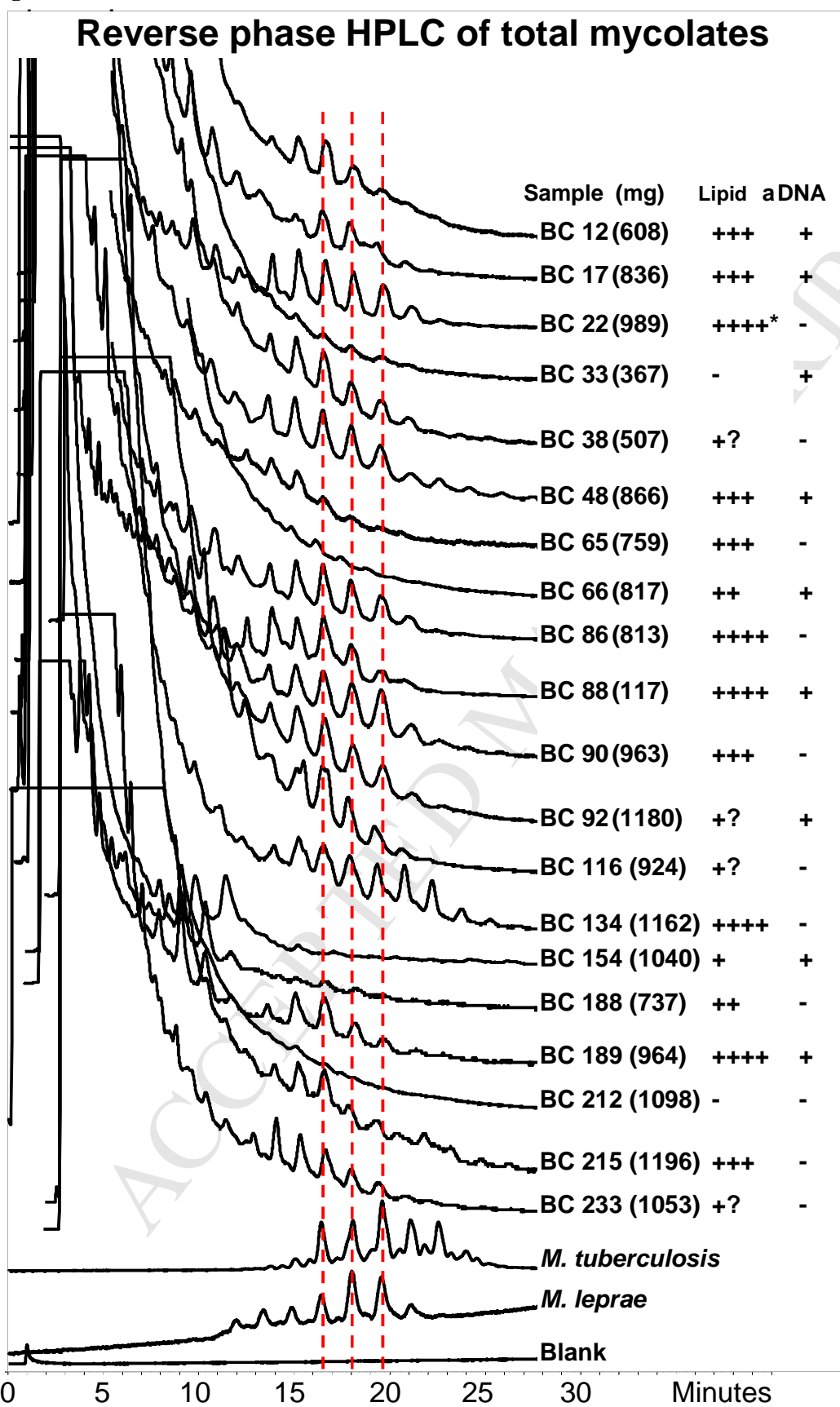
412

21

413 **Figure 2**

414

SUPPLEMENTARY DATA

Paleopathological analysis

The distinction between classical and atypical or early-stage TB cases is shown in the figures below.

Legend to Figure S1

Classical TB cases

a) Tuberculous spondylitis healed with gibbus formation (L1-L3) - Grave No. 65. (female, mature)
b) Severe destruction of the 3rd vertebral body (inferior view) - Grave No. 65. (female, mature)
c) Lumbosacral tuberculosis: severe erosion of the ventral sacral surface (traces of cold abscess) - Grave No. 90. (male, elderly)
d) *Coxitis tuberculosa*: complete destruction and remodelling of the acetabulum - Grave No. 90. (male, elderly)

a)

b)

c)

d)

Legend to Figure S2
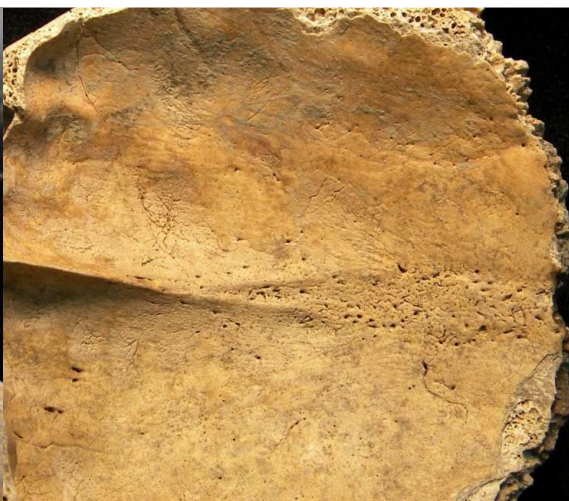
Atypical or early-stage TB changes

a) Periosteal apposition on the visceral costal surface – Grave No. 88. (female, mature)
b) Maze like surface excavation (*serpens endocrania symmetrica*)- Grave No. 233. (female, young adult)
c) Abnormal vertebral vascularisation - Grave No. 92. (male, young adult)

a)

b)

c)

Details of DNA extraction

(a) Disaggregation of samples and DNA extraction

A small quantity (22–78mg) of each sample was crushed by a sterile pestle in a mortar and added to 400μl of Proteinase K/EDTA. Samples were processed in batches of 7 plus a negative extraction control. The slurry was incubated at 56ºC[24], and mixed on a bead beater daily. When the sample was solubilised, it was divided and one aliquot treated with 40μl of 0.1mol [1] of N-phenacylthiozolium bromide (PTB), to cleave any covalent cross-links thus enabling DNA strand separation and amplification[21]. Sample tube contents were transferred into separate 9ml tubes of NucliSens® (bioMérieux) lysis buffer containing 5mol [1] guanidium thiocyanate and incubated for 1–3 days at 56ºC. To complete the disruption of bone and any mycobacterial cell wall remnants, samples were boiled, then snap-frozen in liquid nitrogen and thawed in a 65ºC waterbath. This procedure was repeated twice. Sample tubes were centrifuged at 5000g for 15 min at 5ºC and the supernatants carefully removed into clean, sterile tubes. DNA was captured by adding 40μl silica suspension (NucliSens®) and mixing on a rotator wheel for 1 h. Tube contents were centrifuged and silica pellets washed once with wash buffer (NucliSens®), twice with 70% (v/v) ethanol (20ºC) and once with acetone (20ºC). After drying in a heated block, DNA was eluted using 60μl elution buffer (NucliSens®), aliquoted and used immediately or stored at 20ºC. Silica supernates (500μl) from PTB-negative samples were also collected from the 9ml tubes of lysis buffer, and the 2.0ml screw-capped Eppendorf tubes used to wash the silica. After chilling at 5ºC, supernates were mixed vigorously for 20 s with 200μl of Protein Precipitation Solution (SLS Ltd., UK) and centrifuged for 3min at 10,000g. Any pellet was discarded and 600μl isopropanol (20ºC) added to 550μl of each supernate. Tubes were mixed by inversion 50 times and spun 3min. Supernates were discarded and tubes washed once with 500μl 70% ethanol (20ºC). After draining, tubes were dried in a heating block. Any precipitated DNA was re-hydrated with 60μl elution buffer (NucliSens®), aliquoted and used immediately or stored at 20ºC. Negative extraction controls were processed in parallel with the test samples.

(b) DNA amplification and detection

Two specific regions of the MTBC were targeted in the repetitive elements IS6110 (1–25 copies/cell) and IS1081 (6 copies/cell). The IS6110 primers had a target region of 123 bp[22] and the IS1081 primers designed by Taylor *et al.*[23] produce an amplicon of 113 bp. Later,

specific *M. tuberculosis* primers and a fluorescent probe were used[24] to enable shorter DNA fragments to be detected in a real-time PCR reaction.
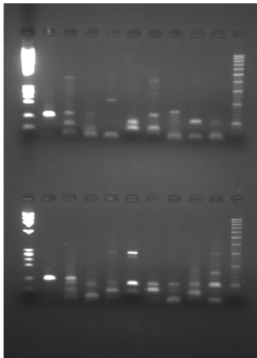
(c) The PCR conditions

The PCR mix included 2mM bovine serum albumin (BSA) to reduce PCR inhibition[25] and 2.0mM $MgCl_2$. PCR assays were initially run at an annealing temperature of 58ºC and amplified DNA was examined by agarose gel electrophoresis.[26] Subsequently, amplification was performed in a final volume of 25μl using a RotorGene© 3000 (Qiagen) real-time platform[27], to enable the detection of DNA using SYBR Green and melt analysis or specific primers with fluorescent probe. Annealing was at 60ºC. A hot-start Taq polymerase was used to minimize non-specific primer and template binding. Negative DNA extraction and PCR controls were processed alongside the test samples.
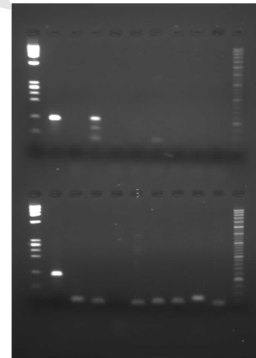
(d) Results

Single-stage PCRs with outer primer pairs

Gel with IS*6110* PCR products   Gel with IS*1081* PCR products

Key to abbreviations:
EC = negative extraction control; s = silica supernate (fluid left in 2 ml tubes after silica spun down, normally short aDNA fragments); LVs = large volume silica supernate (fluid left in 9 ml lysis buffer tubes after silica spun down, short aDNA fragments); wb = water blank negative control in PCR.

Lanes (left to right): 1: Phi X-174 *Hae*III markers; 11: 20bp and 100bp molecular markers

Top row: 2: +ve control; 3: BC-12s; 4: BC-12 LVs; 5: wb1; 6: BC-17s; 7: BC-17 LVs; 8: BC-22s; 9: wb2; 10: BC-22 LVs;

Bottom row: 2: +ve control; 3: BC-33s; 4: BC-33 LVs; 5: BC-38s; 6: ECs; 7: BC-38 LVs; 8: BC-48s; 9: BC-48 LVs; 10: EC LVs;

Conclusions:
IS*6110*: possible weak positives with BC-12 LVs and BC-17 LVs. Positive with BC-33s. Non-specific bands from BC-12s, BC-22s, BC-33 LVs, and BC-48 LVs. Others negative.
IS*1081*: positive with BC-12 LVs. All other samples (except positive controls) were negative

Single-stage IS*1081* PCRs using inner primers (113 bp)
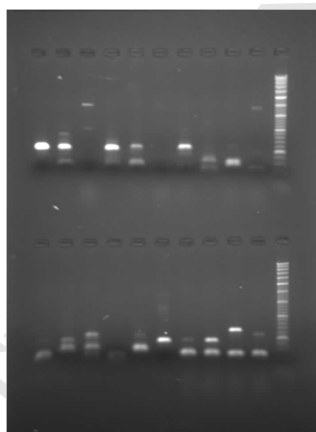
Lanes (left to right): 11: 20bp and 100bp molecular markers
Top row: Lane 1: +ve control; 2: BC-12; 3: wb5; 4: BC-12+; 5: BC-17; 6: wb6; 7: BC-17+; 8: BC-22; 9: BC22+; 10: wb7.
Bottom row: Lane 1: BC-33; 2: BC-33+; 3: BC-48; 4: wb8; 5: BC-48+; 6: EC; (lanes 7–10: different samples and another PCR)
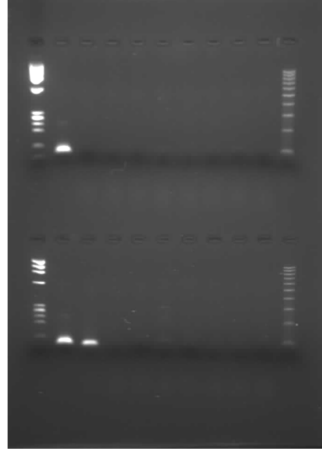
Conclusions:
Positives from samples BC-12, BC-12+, BC-17, BC-17+, BC-48.
Doubtful results from BC-22, BC-22+ (very faint trace) and BC-48+.
Negatives from BC-33 and 33+, and all water blanks.
BC-51 was examined separately for MTB *IS1081* but was negative.

Nested IS*6110* PCRs using inner primer pair

Samples loaded in the same order as above, using the stage 1 PCR products that were re-amplified for a further 25 cycles.

Conclusions:
Positive and negative controls were satisfactory. Only BC-33s was positive.

Real-time experiments were also carried out with the same primers and melt analysis. Results are summarized at the end of the document.

Real-time PCR with IS*1081* primers and probe
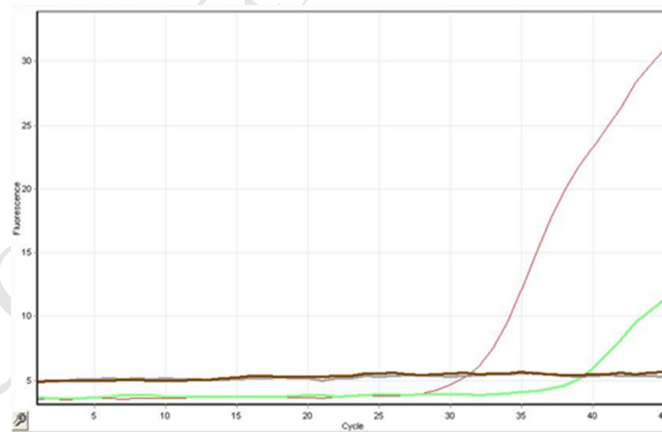
The lower the cycle threshold (C_t) the greater the quantity of target aDNA in the sample. In this image, the positive samples in order of their C_t was as follows:

Positive control (a 1/10 dilution of extract from a Vác mummy) C_t 32 cycles
BC-189+ (+ indicates the DNA was extracted using PTB) C_t 39 cycles
Negatives were obtained from BC-12, BC-22, BC-116+, BC-116, BC-134+, BC-134, BC-134s, BC-188+, BC-188, BC-189, BC-215, wb1, wb2, wb3, wb4, EC, EC1, EC+, ECs
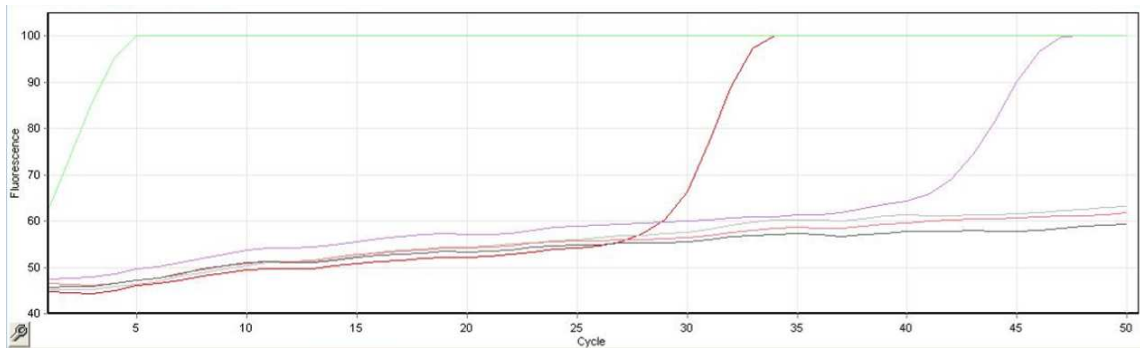
In this experiment a nested PCR was performed on the PCR product from BC-189+ which explains the high level of signal at the start of the reaction. The positive control had a C_t of 28 and sample BC-92 had a C_t of 41.

Negatives were obtained from BC-22, BC-65+, BC-65, BC-66+, BC-66, BC86+, BC-86, BC-88+, BC-88, BC-90+, BC-90, BC-92+, BC-154+, BC-154, wb1, wb2, wb3, wb4, EC+, EC.
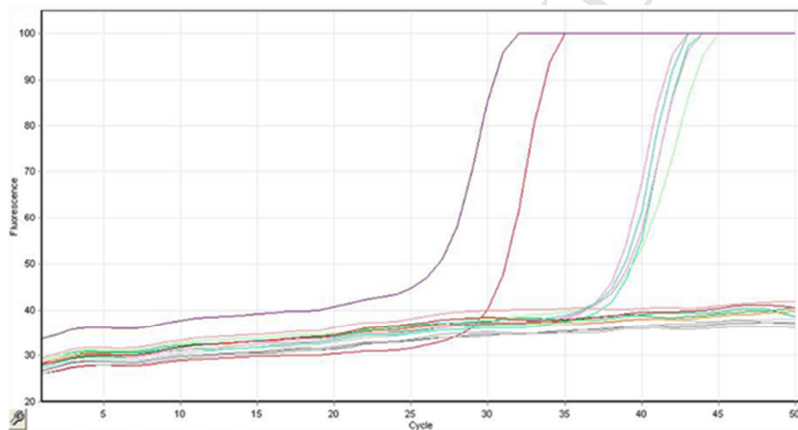
The positive control had a C_t of 28.6, BC-66s: 36.6, BC-86s: 36.9, BC-92: 36.0, BC-92s: 36.3, and BC-154: 36.1. Individual screenshots are available for each positive sample.
Negative results were obtained from BC-65s, BC-86s, BC-90s, wb, EC and ECs.
These results were confirmed by agarose gel electrophoresis.

Overall findings for M. tuberculosis *complex in these samples*
Positives with one or both target regions:
BC-12, BC-17, BC-33, BC-48, BC-66, BC-88, BC-92, BC-154, BC-189
Negative (but cannot exclude poor preservation):
BC-22, BC-38, BC-65, BC-86, BC-90, BC-116, BC-134, BC-188, BC-212, BC-215, BC-233

9

Analysis of mycolipenate and mycocerosates

The initial analyses were performed at Bristol University, using a ThermoFinnigan MAT95 XP-Trap mass spectrometer, fitted with a Phenomenex Zebron ZB-5 (5% phenyl, 95% dimethylpolysiloxane) capillary column (30 m × 0.25 mm i.d. × 0.25 µm film thickness) using He as carrier gas (constant flow mode 1ml min^{-1}) and ammonia as the CI reagent gas. A GC oven temperature gradient from 200 to 300ºC at 6.7ºC min^{-1} was used, the final temperature being held for 20 min. The ion source temperature was 250ºC, the injector 300ºC and the transfer line 300ºC. Selected ion monitoring (SIM) was used for mycocerosate ions at m/z 367.6311 (C_{24}), 395.6844 (C_{26}), 409.7111 (C_{27}), 437.7645 (C_{29}), 451.7911 (C_{30}), 479.8445 (C_{32}), 493.8712 (C_{33}) and 507.8978 (C_{34}); additionally, m/z 407.6952 was monitored for the presence of C_{27} mycolipenic acid. Later studies were carried out at Swansea University with the same Phenonemex Zebron ZB-5 column, using He as carrier gas. PFB esters, on NICI-GCMS, fragment to produce negative carboxylate [M – H]$^-$ ions, which can be detected at high sensitivity. Selected ion monitoring (SIM) was used to search for mycocerosate carboxylate ions at m/z 367.6311 (C_{24}), 395.6844 (C_{26}), 409.7111 (C_{27}), 437.7645 (C_{29}), 451.7911 (C_{30}), 479.8445 (C_{32}), 493.8712 (C_{33}) and 507.8978 (C_{34}).[29] Additionally, m/z 407.6952 was monitored for the presence of the C_{27} mycolipenate carboxylate ion.[29] Partial racemisation of mycocerosates during the alkaline hydrolysis leads to the formation of diasteroisomers, which resolve on gas chromatography to give characteristic doublets; in contrast, mycolipenates are singlets as they cannot racemise.[29]

Legend to Figure S3

Selected ion monitoring (SIM) negative ion chemical ionisation (NI-CI) gas chromatography mass spectrometry (GC-MS) of pentafluorobenzyl esters (Swansea University). **A.** Standard *M. leprae* (Swansea University); **B-H.** Samples extracted from graves (BC) 22, 12, 17, 33, 38, 65, 66, respectively. Intensities (**bold in brackets)** are normalised to the major component **(100).**
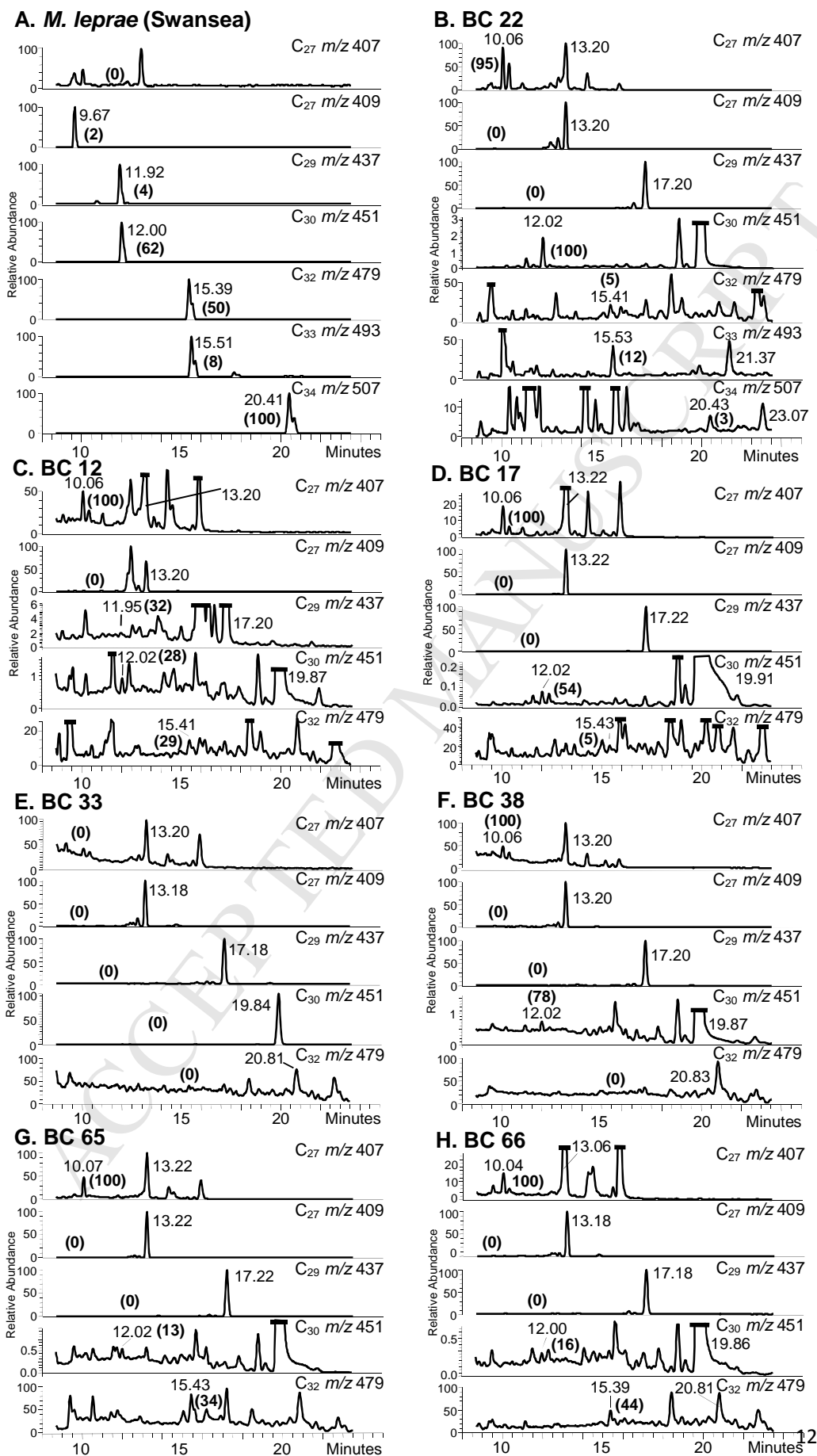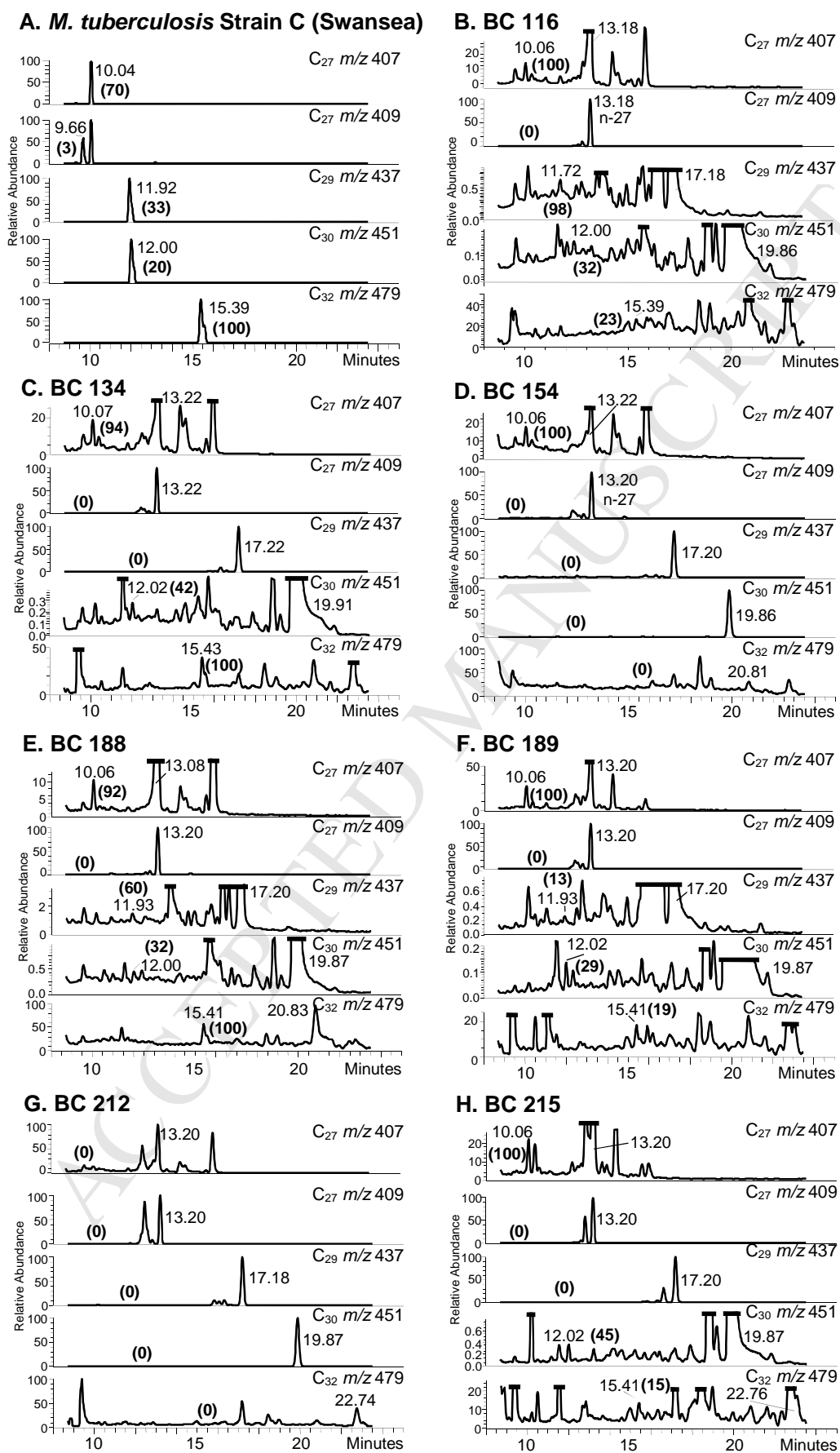
Figure S3

Legend to Figure S4

Selected ion monitoring (SIM) negative ion chemical ionisation (NI-CI) gas chromatography mass spectrometry (GC-MS) of pentafluorobenzyl esters (Swansea University). **A.** Standard *M. tuberculosis* (Strain C) (Swansea University); **B-H.** Samples extracted from graves (BC) 116, 134, 154, 188, 189, 212, 215, respectively. Intensities (**bold in brackets)** are normalised to the major component **(100).**

Figure S4

A. *M. tuberculosis* Strain C (Swansea)

B. BC 116

C. BC 134

D. BC 154

E. BC 188

F. BC 189

G. BC 212

H. BC 215

14

Legend to Figure S5

Selected ion monitoring (SIM) negative ion chemical ionisation (NI-CI) gas chromatography mass spectrometry (GC-MS) of pentafluorobenzyl esters (Bristol University). **A-F.** Samples extracted from graves (BC) 48, 86, 88, 90, 92, 233, respectively. Intensities (**bold in brackets)** are normalised to the major component **(100).**

Figure S5

A. BC 48

B. BC 86

C. BC 88

D. BC 90

E. BC 92

F. BC 233